PANORAMA of the UNIVERSE

A

Cylindrical Reflector SKA

Concept Extension & Responses to EMT/ISAC

John Bunton, Duncan Campbell-Wilson, Anne Green, Carole Jackson, Mike Kesteven, Andrew Parfitt and Elaine Sadler

Editor John D. Bunton

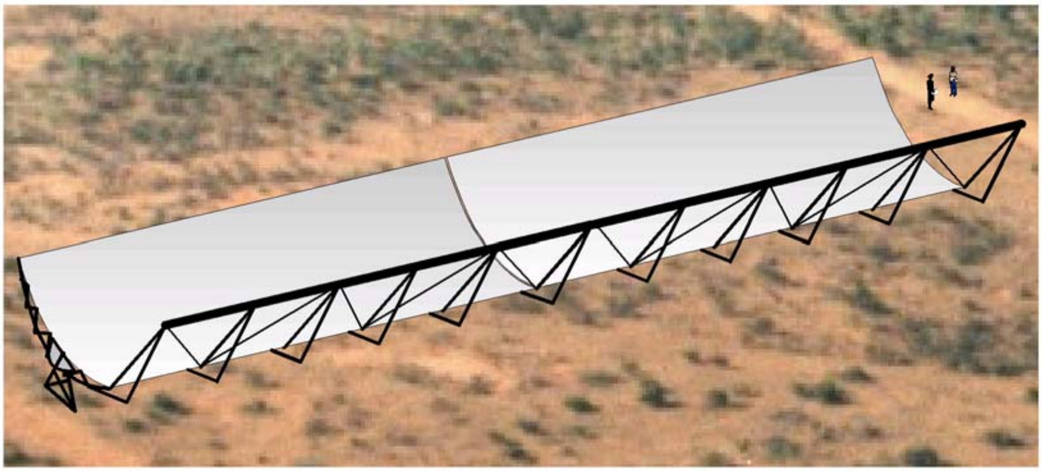

Submitted by the Australian SKA Consortium
May 2003

SKA
SQUARE KILOMETRE ARRAY

Executive Summary

This update to the cylindrical reflector white paper [1] further explores the possibilities of the concept as well as refining the cost estimates. The cost of the line feed and its associated electronics has been significantly reduced largely through the use of ASICs (application specific integrated circuits). This has allowed the maximum frequency to be increased to 22 GHz for a total cost of 1.3 billion US dollars, which includes civil engineering, cable trenching, computing and non-recurring engineering costs.

The major technical improvement is the modification that allows bandwidth to be traded for field of view (FOV), allowing the imaging FOV at 1.4 GHz to be increased to 48 square degrees. This opens up the exciting possibility of carrying out an all-sky survey at 1.4 GHz to a limiting sensitivity of 10 μJy in less than 12 hours. Such a survey would provide radio images with one arcsec resolution that would go deeper than ANY radio continuum image so far made, and would not only cover the entire sky but could be repeated every day. Such a survey would open up new parameter space in both sensitivity and time resolution, allowing new science to be done in the areas of GRBs, radio supernovae, pulsars and other transient objects.

Even at 22 GHz the cylindrical reflector is fast. When compared to a 12 m antenna it can access 23 times the sky area and image 4.6 times more sky in the same time. At 1.4 GHz the imaging capability is 30 times greater than a 12 m antenna. This makes the cylindrical reflector concept the fastest of the current concepts at frequencies above 1.5 GHz. The increase in observing speed is equivalent to approximately a four fold increase in available observing time. This gives either a four fold increase in science throughput or twice the sensitivity: 40,000 m^2/K at 1.4 GHz.

This update addresses specific questions raised by the EMT. Also addressed are numerous technical aspects: non-correlator modes, pencil beams, sampling times, number of IFs, IF separation, subarraying, spectral resolution, central core sensitivity, dynamic range and acquisition speed. This allows all ISAC specifications to be quantified. These are shown together with the current SKA specifications and the most demanding ISAC requirements in the table on the following page. It is seen that the cylindrical reflector can satisfy most science requirements of the ISAC while at the same time providing a high speed instrument with superb surveying capabilities.

© CSIRO

Cylindrical Reflector Specifications and SKA compliance

	Cylindrical Reflector	SKA [7]	Compliance matrix [8]#
Antenna size	110 m by 15m		
A/Tsys			
0.3 GHz (Tsky 60K)	7,400 m^2/K		
1.4 GHz	20,000 m^2/K	20,000 m^2/K	20,000 m^2/K
10 GHz	16,000 m^2/K		
20 GHz (Tsky 20K)	8,200 m^2/K		
double these values if the FOV enhancement is included e.g. 1.4 GHz	40,000 m^2/K		
Frequency range GHz	0.1 to 22	0.15 to 20	0.1 to 36
Antenna Field of View			
1.4 GHz	120^o x 1^o; 120 deg^2		
5 GHz	34^o x 0.28^o; 9.5 deg^2		
10 GHz	5^o x 0.14^o; 0.72 deg^2		
20 GHz	2.5^o x 0.07^o; 0.18 deg^2		
Imaging Field of View			
1.4 GHz (0.8 GHz BW)	48 deg^2	1 deg^2	1 deg^2
5 GHz (1.6 GHz BW)	1.9 deg^2		
20 GHz (full BW)	0.035 deg^2		
No. beams			
Antenna (full BW)	8 to 64		
Antenna (800 MHz BW)	48 to 384		
Tied array (full BW)	400	100	100
Subarraying			
Per 110x15m Antenna	4		>~10
With three subgroups	12		
FOV at 1.4 GHz	600 deg^2		
Response time,			
standard	~60 sec		<~10
optional high speed antenna	<~10 sec		
Correlation and Tied Array			
Bandwidth	4.9 GHz	4.5	8 (=15/2 +0.5)
No. spectral channels	512 to 4096 x 6	10,000	4,000
Spectral resolution, standard	1.5 MHz – 200 kHz		
Spectral resolution, cascaded	100 kHz – 1Hz		1Hz
Sampling time	0.6μs		5μs
IFs			
No. independent	6	2	>10
Max sep. of IFs	14 GHz		24 GHz
Baselines			
Maximum on land	3,000		5,000
with trans oceanic links	10,000		
50% area/baseline	47% within 2km		
Performance			
Spatial DNR @ 1.4 GHz	1.00e+06	1,00e+06	1.00e+07
Spectral DNR	1.00e+05		1.00e+05
Polarization DNR	High (see text Q1)	-40dB	1.00e+04
Number of spatial pixels	>1.00e+09		1.00e+09
Tb sensitivity	See appendix 1		

compiled from the most demanding science (case) specification in the underlying level 1 science cases

© CSIRO

Contents

© CSIRO

Cylindrical Reflector Concept
- Extensions and Clarifications

1.1 Introduction

The concept of a cylindrical reflector based SKA is fully set out in the 2002 white paper, 'Cylindrical Reflector SKA', SKA memo 23 [1]. This document should be consulted for details of the proposal. In brief, the concept provides for 600 cylindrical antennas each 110 m by 15 m, with the axis of rotation oriented EW. This provides full declination coverage with maximum sensitivity at transit. At the focus of each antenna is a linefeed ~100 m in length. Electronic scanning of this linefeed allows sources up to 60^o from transit to be observed. At the scanning limit the sensitivity falls by 3dB. An advantage of the concept is the relatively large field-of-view (FOV). As antenna stations are single filled-aperture antennas full advantage can be taken of the FOV because FOV is maximised for a given signal transmission bandwidth, and correlator costs are minimised. In this document the possibilities provided by this concept are further explored, as well as clarifying numerous technical specifications needed to determine the concept's suitability for the various science cases.

1.2 Revised costs and increase in maximum frequency

The technologies required for line feeds and phased arrays are essentially identical. However, in the 2002 white paper proposals, the cylindrical reflector line feed elements [1] were an order of magnitude costlier than the aperture tile elements [2]. As these elements have essentially the same function the costs should have been similar. The main reason for the difference was the use of FPGAs and discrete A/D converters instead of ASICs for the cylindrical reflector white paper costings. As foreshadowed in the white paper, using ASICS reduces digitising, beamforming and correlator costs but adds to the non-recurring engineering (NRE) costs. An order of magnitude cost reduction is possible, but here a more conservative reduction by a factor of five is assumed.

Other linefeed costs also need to be broken down. Previously the feed element, LNA and RF beamformer were grouped together and a cost proportional to frequency was assumed. This is true of the LNA and RF beamformer but the linefeed hardware itself actually decreases in size with frequency. Thus less material is needed but this is offset by the greater complexity and possibly higher material costs. Here it will be assumed that the antenna cost increases as the cube root of frequency in the same way that reflector costs increase. Further, it is assumed that at 1 GHz the feed elements are as costly as the LNAs and RF beamformers. Based on the white paper costing the new 1 GHz costs are $US115/m for the feed elements, $US115/m for the LNA and RF beamformer, and $US162/m for the down conversion, digitising and digital beamforming with 700 MHz of bandwidth.

These costs can be directly compared to a line feed made from a five-wide linear array of aperture tile elements. At 1.5 GHz this would cost US$175/m based on aperture tile estimates [2]. This line feed cost using aperture tile estimates is a factor of 2.5 cheaper than the revised cylindrical reflector estimates. Further, the linefeed may have passive

© CSIRO

beamforming across five elements and generate a single beam as compared to four for the aperture tile estimates. Thus the revised cylindrical reflector cost is relatively conservative when compared to aperture tile costs.

A further cost reduction is due to the increased bandwidth of the line feeds, possibly up to 5:1 (see answer to Q1 section 2.1). Here a 3:1 linefeed bandwidth is assumed which increases the cost of multiple linefeeds by ~50% when compared to a single high frequency linefeed. This is a 25% cost reduction relative to the original white paper costs which assumed a 2:1 linefeed bandwidth. Thus at 22 GHz the linefeed costs are estimated to be:

- Linefeed hardware US$29M cost proportional to $\nu^{0.33}$
- Linefeed electronics US$229M cost proportional to frequency ν plus
- Down conversion and A/Ds US$43M

Changes to the beamformer have increased the cost in the fibre link between the line feed and the beamformer. This is further discussed in the answer to Q3 (section 2.3) where the cost is estimated to add US$12M per GHz of processing bandwidth. A single centralised beamformer is now used for each antenna which increases the available FOV.

For a complete cost estimate, civil engineering, computing and NRE costs must be added. The original white paper estimate included the cost of foundations and much of the cabling costs as the data used for the estimates came from complete antenna designs. However site acquisition, power, roads and buildings should have been included. To estimate added civil costs, the US white paper estimate [14] has been taken and foundations and most of the cabling costs removed. The estimated added civil engineering costs are US$100M.

Finally, computer hardware, programming and NRE costs must be added. This has been estimated at US$190M in the US proposal [14]. These costs should be similar for the cylindrical and the US 12 m proposal. Their cost is therefore adopted as the estimate to be used here. This cost provides for functions such as control, monitoring, processing, and image formation as well as non-recurring design, integration, testing, and management. When added to civil engineering costs, and inter-station cable and trenching it is seen that fixed costs come to US$440M. Including these fixed costs and using the new linefeed and correlator cost results in the cylindrical reflector estimates shown below.

Table 1 Revised estimated cylindrical reflector estimated cost including full civil, computing and NRE costs. (A/Tsys ~ 20,000 for frequencies from 0.5 to 10 GHz).

Maximum Frequency GHz	3	6	9	12	15	22	32
Correlator bandwidth GHz	1.1	1.7	2.5	2.9	3.5	4.9	6.9
Revised cost estimates US$M	752	865	961	1050	1134	1319	1569

If the adjusted linefeed and correlator costs are achieved the cylindrical reflector concept is competitive up to a frequency of 22 GHz. The cost breakdown is shown below

© CSIRO

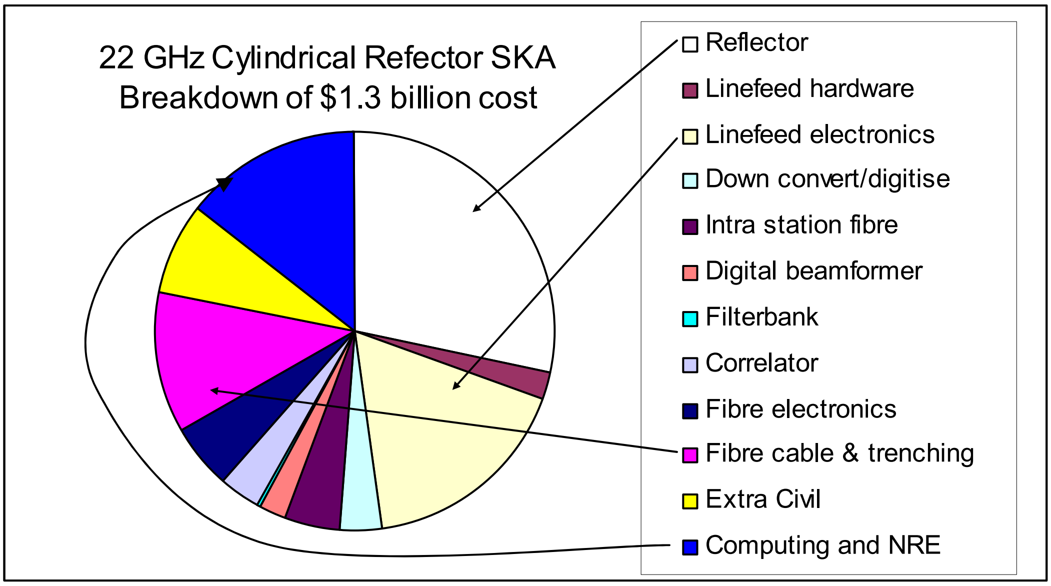

Figure 1 Estimated cost for a 22 GHz cylindrical reflector SKA

The EMT has also asked for the specification possible with US$1 billion limit on the cost. From the above table it is seen that a full specification 12 GHz instrument could be built. Increasing the frequency to 22 GHz could be achieved in a number of ways.

As ~US$500 million of the cost of a 22 GHz instrument is due to electronics, costs are reduced by waiting for Moore's law to bring the cost of processing power down. By 2012 the cost of electronics is potentially halved to US$250 million. However, part of the electronics cost such as cables and power supplies does not decrease as rapidly so the saving is about US$200M. A further US$100M could be saved by reducing the number of antennas from 600 to 534 bringing the total cost down to US$1 billion.

An alternative to waiting for Moore's law is to reduce the high frequency collecting area. If only half of the array is equipped with 7-22 GHz linefeeds and accurate 22 GHz surfaces the linefeed cost is reduced by a third. The reflector cost is also reduced and the signal transport and processing load is halved reducing the cost to US$1065million. The effect of this is to halve the high frequency sensitivity and halve the low frequency FOV (because the total transmission bandwidth is reduced). However, when the speed of the concept is considered the effective high frequency A/Tsys is still ~8,000 m^2/K at 22 GHz.

1.3 System temperature

For a fixed A/Tsys approximately two thirds of the cost of the SKA is directly proportional to system temperature. The white paper [1] assumed 30K with 5K margin for error. However, sky noise was underestimated and inter element coupling, estimated at 2K, was not included. This increases the estimated Tsys to 33K which is still within the 35K allowed. To achieve this, a 14K LNA noise temperature is needed. This was based on an extrapolation from the Infineon BFP620 performance, 51K at 1.8 GHz uncooled. It appears that this extrapolation is still on track. Performance of Infineon devices continues to improve with the release of the BFP640, 47K at 1.8 GHz.

© CSIRO

A SiGe device from Toshiba [3] does even better, 37K at 2 GHz. This is a 14K decrease in a period of two years.

SiGe transistors can be left unmatched and still have a noise temperature close to that of the transistor alone. Confirmation of this is seen with a sample amplifier built at CSIRO using a BFP620 that measured 47K at 1.8 GHz [4] with 50 ohm loads. As there is no matching, the device is inherently broadband, operating from 100 MHz to 6 GHz. The effect of antenna mismatch is still to be explored. Experimental devices have also improved with a new IBM device [5] achieving a claimed uncooled spot noise temperature of 14K at 11 GHz. Independent confirmation of this result would show that SKA requirements have already been met at frequencies up to 11 GHz.

The IBM experimental device had a 200 GHz transition frequency with a 350-400 GHz device under development. This is three to six times higher than the 65 GHz Infineon devices. If performance scales with transition frequency then a 400 GHz Infineon device should have a noise temperature of 47K at 11 GHz. By 2010 a noise temperature of at most 47K at 22 GHz should be achievable for SiGe. The Toshiba device would indicate that 37K is possible. However, other losses will be higher in a 22 GHz system, including about 20K of sky noise. The estimated SKA system temperature is 85K and the corresponding SKA sensitivity is 8200 m^2/K. At 10 GHz the sky noise is negligible and LNA noise temperature should halve giving an estimated SKA sensitivity of 16,000 m^2/K. These estimates currently have a high degree of uncertainty.

1.4 Bandwidth – FOV trade-off

As will be seen in the reply to Q3 from the EMT (section 2.3) there is a trade-off between bandwidth and FOV. Full advantage of this trade-off can be made if all digitised signals are combined in a single beamformer. The FOV available within these signals is the antenna FOV. The centralised beamformer adds to the cost of intra-antenna signal transport but allows beams to be formed anywhere within the antenna FOV.

Table 2 Antenna beamwidths as a function of operating frequency *f* GHz

	0.1 to 1.5 GHz	1.5 to 7 GHz	above 7 GHz
MD coverage deg	120	$170/f$	$51/f$
Reflector beamwidth deg	$1.4/f$		
Bandwidth GHz	1.6	1.6	4.9

The output of the beamformer is constrained by inter-station transmission bandwidth. This reduces the total FOV. When the linefeed is fully beamformed it is possible to simultaneously correlate all the transmitted data allowing full imaging. Thus the FOV embodied in the signals transmitted from the antenna will be referred to as the imaging FOV. Imaging FOV as a function of frequency for a number of different bandwidths is shown below.

© CSIRO

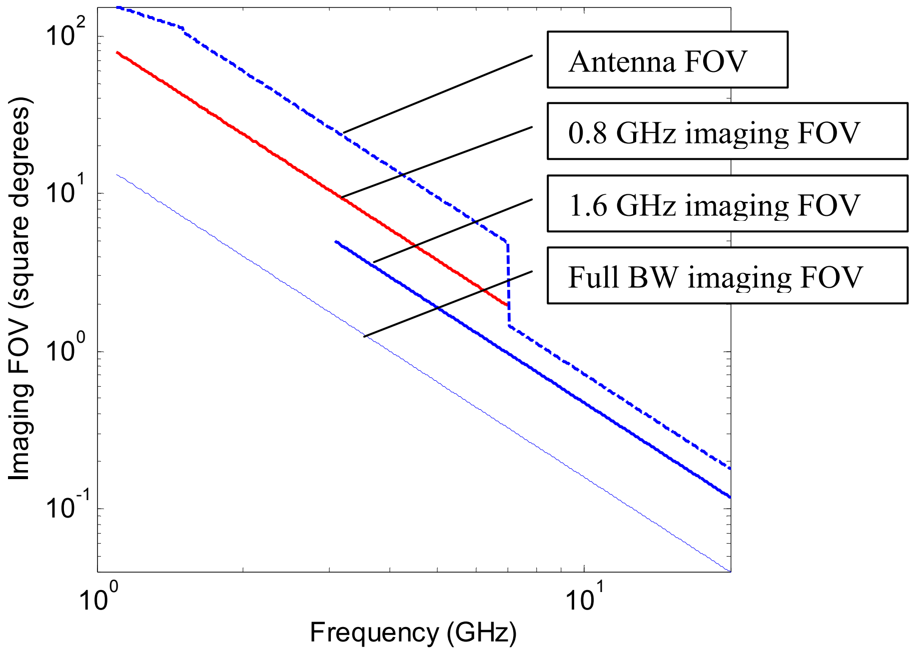

Figure 2 Fields of view for the cylindrical concept

1.5 Subarrays

Subarraying can be accomplished by dividing the antennas into a number of subsets. Many subarrays are possible for baselines up to 30 km. However beyond about 30 km using more than two or three subsets will start to compromise UV coverage.

Further subarraying is achieved by individually pointing the subsection of the antenna. The current design specifies that the 110x15 m reflector be built in a number of sections, probably four. Each of these can be pointed at different declinations providing four independent subarrays per antenna station. Preferentially the centre sections should point to sources within about 30^{o} of transit. The western section of the antenna can observe a source before transit without decreased efficiency and the eastern section provides coverage after transit. Observing outside these preferred ranges is still possible but with reduced sensitivity. The area of sky accessible and the number of antenna beams available is shown in the table below, total number beams is limited by antenna to correlator bandwidth. If necessary all these beams can be imaged.

Table 3 Total FOV at 1.4 GHz and number of antenna beams for different subarraying modes.

	Full sensitivity FOV	Accessible sky	No. full BW beams	No. 800 MHz beams
Antenna operated as 4 separate sections	200 sq deg	480 sq deg	64	384
Antennas in 2 subsets	400 sq deg	960 sq deg	64	384
Antennas in 3 subsets	600 sq deg	1440 sq deg	64	384

© CSIRO

1.6 Non-correlator modes – pencil beams and high time resolution

The original white paper did not address non-correlator modes, but it did stress that data for the full bandwidth on all beams are available at the correlator. Here the signals can be beamformed. These signals are already correctly delayed and have passed through a filterbank. Beamforming requires a single complex multiply and addition per signal. Using SKAMP stage I costs for the complex multiply gives a current cost of US$250k per beam per GHz for a 4-bit FPGA implementation. By 2010 the cost would be about US$10k per GHz. A 100 pencil beam 5 GHz bandwidth implementation would cost ~US$5M. These pencil beams can be placed anywhere within the FOV of any of the 8 circular antenna beams. A total of 400 pencil beams are possible when the antenna is operated with 64 fanbeams. Reducing the bandwidth to 800 MHz increases the number of pencil beams to 2400. Up to 2400 pencil beams can provide a high time resolution signal with full SKA sensitivity. The time resolution depends on the resolution of the filterbank. With a 512 channel 800 MHz filterbank the time resolution is 0.6μs.

1.7 Acquisition Time

Both SETI and transient phenomena science groups ask for response times less than 10 seconds. Antennas with a slew rate of ~2^o per second can provide access to a 40^o by 120^o section of sky (~1.5 steradians) in 10 seconds. If this is too costly then only a subset of antennas would be outfitted with the fast slew rate drives.

If high speed access to most of the available sky is necessary then the array can be set up with three groups of high speed antennas. The transit declinations of the groups must be spaced about 40^o apart; this prevents two of the groups from contributing to normal SKA operations. These additional antennas would be an additional cost to be added to the budget.

1.8 Central core

The specification for Epoch of Re-ionisation science requires 50% of the total area to be within 2 km. In the current design there are 250 antennas in the central 2 km and 32 further antennas that, correlated with the central core have baselines less than 2 km. This corresponds to 47% of full sensitivity for baselines up to 2 km. To achieve 50% within 2 km would increase the SKA cost by 3% and increase the total sensitivity, at all baselines, by 6%. Alternatively, the 3000 to 10,000 km trans-oceanic baselines could be sacrificed and these 33 antennas placed within the central core.

1.9 Number of IFs, IF separation and dynamic range

The original white paper suggests three 800 MHz IFs. With the maximum frequency increased to 22 GHz, six IFs per polarisation are needed. The increased maximum frequency relies on the use of Radio-on-a-chip technology which allows considerable flexibility. Each IF is to be processed by a 512 to 4096 channel digital filterbank with better than 60dB stopband attenuation with spectral resolution of 1.6 MHz to 200KHz.. Higher spectral resolution, 100 kHz to 1 Hz, will rely on cascaded filterbanks [6]. Estimated spectral line dynamic range is 50 dB (1.0e5 in power) requiring 8-10 bit A/D

© CSIRO

converters and care in reducing intermodulation distortion in the RF and IF chain. This dynamic range will also make the system robust to interference.

If more than 4.9 GHz of processing bandwidth is required, extra down conversion and digitising hardware is needed. However with suitable input data multiplexing, the same beamforming, filterbank, signal transmission and correlator hardware can be used. The compromise is then to halve the total number of beams and image size. A doubling of the available bandwidth to 10 GHz is estimated to cost US$50M. This requires local digital beamforming on the linefeed; otherwise an additional US$60M in optical fibre interconnection is needed.

On the highest frequency linefeed a number of independent IFs are needed. If this linefeed covers a 3:1 frequency range the IF separation can be up to 14 GHz. With a 4:1 frequency range linefeed it becomes possible to do geodesy using the frequencies 5 and 20 GHz. If IFs on other linefeeds are also considered, the frequency separation can encompass the full frequency range. However, the degree of overlap between the FOVs of the different linefeeds will only be determined when practical designs are simulated and constructed.

1.10 Update on SKA Molonglo Prototype (SKAMP) project

The aims of the SKAMP project are to develop and test SKA-relevant technologies on cylindrical reflectors and to provide a new capability for low-frequency radio astronomy in Australia based on the Molonglo Observatory Synthesis Telescope. The project has now been split into three stages for efficient implementation. Stage 1 is to equip the current telescope, which operates in the radio continuum at 843 MHz, with a new 96-station 3 MHz-bandwidth correlator as a parallel backend. The heart of this stage is an FX correlator, which has now been designed and about to be sent for manufacture. The delay units and data acquisition systems are nearing completion. A PhD student is currently working on imaging problems posed by the data from this correlator.

Stage 2 will deliver a 30 MHz bandwidth spectral line capability, centred on 843 MHz, using the existing front end system of the telescope. It is expected that the young engineer working on the correlator will commence a PhD to design the scaled up correlator. An industry Linkage project grant between the University of Sydney, CSIRO and Argus Technologies is funding the development of an ultra wide-band feed system for the cylindrical paraboloids which will be installed on the telescope in Stage 3, broadening the instantaneous bandwidth to 100 MHz and increasing the frequency coverage to 300 to 1420 MHz. The feed development project supports a PhD student and a Postdoctoral Fellow for three years. The timescale for the completion and commissioning of the SKAMP project is 2007. The stages of the project are summarised below.

- Stage 1 2003 a 96 station continuum correlator using existing 3 MHz IF
- Stage 2 2005 a 30 MHz spectral line correlator at 843 MHz
- Stage 3 2007 a 300 to 1420 MHz linefeed, and 100 MHz spectral line correlator.

© CSIRO

2 Compliance with Science Group Requirements

The ISAC science groups have evaluated all proposals and the results are summarised in a compliance matrix [15]. Each concept was rated from a positive yes (5) to a positive no (0) for the 18 science cases. Here the specifications presented for the cylindrical concept in this update are compared to the science requirements. In each case, a revised rating is suggested.

2.1 Science Group 1: Milky Way and Nearby Galaxies

The cylindrical concept is already fully compliant (Score of 5) for **Galactic HI**. For **Galactic non-thermal emission and magnetic fields** the cylindrical concept scored a provisional yes (4). The increase in upper frequency now allows the full 1-10GHz frequency range to be covered. Also, with a correlator generating 10^7 correlations, only ~100 integrations (where the correlations are independent) are required to obtain the 10^9 correlation needed to meet the spatial pixels requirements in a map dominated by confusion. This suggests that the compliance score should be increased from 4 to 5.

2.2 Science Group 2: Radio Transients, Pulsars and SETI

This group has set a common specification for all three science areas. Special requirements given include tied subarrays, instantaneous access to FOV, real time baseband signals and care with RFI excision. These matters are dealt with in this document. The transient buffer is not included; this is a backend subsystem that can be added to all proposals which provide real time baseband signals. Other specifications that are now met are frequency range, sampling time, IF separation, spectral and polarisation DNR, and spectral channels. The number of IF is less than the required 10 but the "number may be lower if bandwidth of IFs sufficiently large". The 800 MHz IF bandwidth would appear to meet this. The cylindrical concept still does not fully meet response time (<~10 seconds) and correlation bandwidth (0.5 +f/2). In terms of response time the cylindrical concept accesses 1.5 steradians in 10 seconds which is four times more than any of the other single beam concepts with the same slew rate. With a maximum frequency of 15 GHz the science group asks for a correlation bandwidth of 8 GHz. The cylindrical concept bandwidth is just over 60% of this. The level of compliance shown suggests that the cylindrical concept be given a score of 4 or more for **SETI** and **Pulsars**. For **radio transients** a score of 5 is suggested because of the possibilities opened up by daily all sky surveys.

2.3 Science Group 3: Epoch of Reionisation

The original white paper specifications were fully compliant except for 50% of baselines being within 2 km. For the cylindrical reflector concept there are currently 47% of baselines within 2 km and only small changes are needed to meet this specification. This is possible because of the high filling factor (~0.3) that can be achieved with cylindrical reflectors. The 15 m with of the reflector also gives it the best low frequency performance of the small D concepts suggesting a compliance score of 5.

2.4 Science Group 4: Galaxy Formation

The cylindrical reflector is now fully compliant with this science group's requirements for **HI surveys, and Large-Scale structure and Cosmology and CO surveys**. For **Continuum Surveys** all but the spatial dynamic range of 10^7 is met. It may be that the high correlation count of the cylindrical concept will provide sufficient redundancy and

© CSIRO

UV coverage for this level of dynamic range to be achieved. But, it will need simulations and experience with real cylindrical reflector data before this level of performance could be confirmed. However, it should be noted that the high speed of the cylindrical concept will allow significantly more deep-field mapping than other concepts leading to a boost in the possible science outcomes. A compliance score of 5 is suggested for all three categories.

2.5 Science Group 5: Active Galactic Nuclei

The cylindrical concept already scores 5 for **High-redshift AGNs**. For **the inner regions of AGNs** it failed to cover the 0.3-22 GHz frequency range. This has now been achieved and the cylindrical concept appears to be fully compliant suggesting it be given a score of 5.

2.6 Science Group 6: Protoplanetary Systems

The cylindrical concept now covers the frequency range up to 22 GHz and appears to be fully compliant with the requirements for observing **Protoplanetary Systems**.

2.7 Science Group 7: CMEs and Solar System Bodies

The increase in frequency range and correlator bandwidth proposed in this update makes the cylindrical concept fully compliant with the requirements for observing **Solar System bodies**. This suggest the compliance score should increase to 5. For Coronal Mass Ejections the frequencies below 100MHz will be difficult to achieve but the large width of the reflector relative to other small D concepts puts the cylindrical reflector at a relative advantage. This suggests a possible increase in the compliance score. However to fully meet the specifications hybrid designs may be needed.

2.8 Science Group 8: The Intergalactic Medium

The cylindrical concept already scores a 5 for **non-thermal IGM**. For **thermal IGM** observation compliance has increased but still fails to reach the maximum frequency of 36GHz specified. It is therefore suggested that the score be brought in line with the score for LAR: 4.

2.9 Science Group 9: Space tracking and Geodesy

Space tracking at 32 GHz is still not achieved which would leave the compliance unchanged. For **geodesy** 8 and 32 GHz observations are still not possible but the increased frequency may allow observations at 5 and 20 GHz or 4 and 16GHz. If these bands are sufficient for SKA geodesy then the compliance score would increase to 5, otherwise the score remains 4.

© CSIRO

3 Reply to EMT Questions

3.1 Q1 Line feeds

The wideband, dual-polarization, line feed is a central element of the design. Can the authors give any indication as to how the feed might be realized and what its performance might be, including its performance with hour-angle scan?

The term "line feed" is probably misleading as it implies a single element linear array solution for each polarization. In practice, for complete reconstruction of the incoming wavefront, an optimally sampled focal plane array will be required. For the cylindrical reflector, this means an array with several elements transverse to the reflector axis, depending on the extent of the focal field, and many elements spaced around ½ wavelength apart along the reflector axis. Passive combining of the elements in the transverse direction is envisaged. There is a considerable amount of work being undertaken in the area of phased focal-plane arrays (refer, for example, to the EU/CSIRO collaborative work in the FARADAY program and the work on the "egg-crate" arrays of tapered slot antennas) aimed at producing broad band (possibly 5:1) dual-polarized arrays matched to the focal field produced by a reflector system. Complementary work aimed at optimizing the noise figure of active systems in this environment is also the subject of current research, and it is likely a compromise solution an be found which selects the sample weights to minimise noise figure subject to reasonable efficiency of field matching in the focal plane.

Earlier work by James and Parfitt [9] showed that the focal region of an offset cylindrical reflector is large, and with modest gain loss several "line feeds" might be accommodated efficiently in a cylindrical reflector design. Consequently it is projected that two or three focal plane arrays, designed for different frequency ranges, might be employed depending on the frequency range of interest. Alternatively, space could be left for future upgrades.

Two aspects of performance have been questioned, and responses are provided here:

1. Polarization. The potential depolarizing effects associated with the reflector geometry are mitigated to a large degree if the polarization sense of the orthogonal receiving arrays is aligned at 45 degrees to the reflector axis. Moreover, since the field is optimally sampled in both polarizations, suitable combining networks should allow two orthogonally polarized channels to be derived with high polarization isolation.
2. Scan performance. The focal plane array proposed for use in the cylindrical reflector is based on technologies developed for two-dimensional aperture plane arrays. In the cylindrical reflector application, however, only one dimension (the long axis) is independently phased, while the other (the short dimension) is weighted to match the focal plane field in the direction transverse to the axis of the cylindrical reflector. Fundamentally, however, the environment in which the array operates is not dissimilar to that of a two-dimensional aperture plane array, except that the beam in one direction is formed by a concentrator. It is expected, therefore, that along the axis of the reflector, the impedance change and scanning characteristics of the feed will be similar to that of the two-dimensional array.

© CSIRO

Consequently, the good scanning performance of the egg-crate configuration of tapered slot antennas is expected to translate into acceptable performance as a cylindrical reflector feed over hour scan angles up to 45 degrees or more off axis. In any case, a Floquet analysis of the reflector/feed combination can be conducted to validate this performance after a suitable focal plane weighting has been derived.

3.2 Q2 Beamforming

Can the authors give an indication of how the delay line RF beamformers might be realized and what performance (e.g. transmission and reflection behaviour) might be expected over the wide bandwidths envisaged?

The line feeds may have a frequency coverage of up to 5:1. This requires a true time delay beamformer which can be implemented as discrete delay steps. The size of the delay steps are determined by the allowable phase error and the maximum frequency of operation. The design is therefore implemented in terms of the wavelength at the maximum frequency λ.

The beamformer combines the signals from 0.3 m of $\lambda/2$ spaced feeds. This corresponds to beamforming two feeds per GHz. The scan angle is $\pm 60^o$ so the total delay range needed at the maximum frequency of operation is $\pm\sqrt{3}.\lambda/4$ per element spacing. For maximum operating frequency of 22 GHz beamforming must be done over 44 feed elements. For simplicity a 4 GHz eight-element beamformer is described here. The delay range needed for the end elements of this array is 0.0λ to 3.0λ. For operations at higher frequencies extra delay elements are needed on the outer feeds.

Switched delay lines

A broadband variable delay can be implemented with switched delay lines, which consist of a pair of SPDT switches that can provide either a straight through connection or switch in a delay element as is shown below.

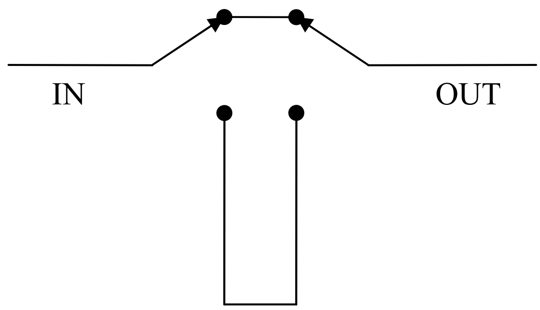

Figure 3 Basic Switched delay element

The standard implementation uses a cascade of these elements where the delay of successive elements is different by a factor of two. For delay range of 3.0λ in steps of 0.20λ a cascade of 4 elements is needed. If a SP4T switch is used a quad delay element can be built and the number of cascaded elements halved. The circuit of the quad delay element is shown below. The delays available are 0, Δ, 2Δ, and 3Δ, after subtracting the minimum delay. This is the same range of delay as is available from a cascade of two switched delay elements with delays Δ and 2Δ. If the switches for the two different implementations have identical performance then the quad delay element has half the loss of an equivalent cascade of two basic elements.

© CSIRO

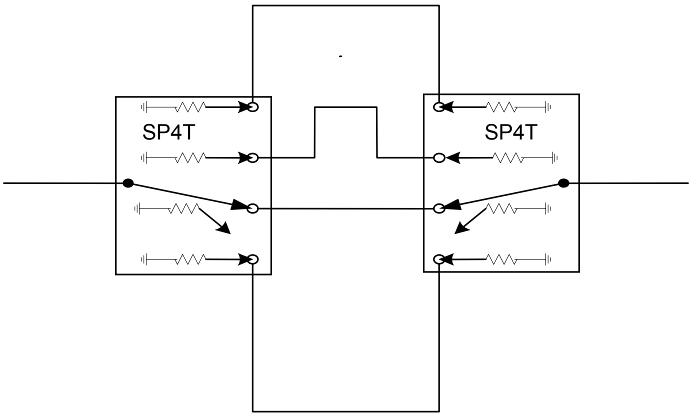

Figure 4 Quad delay element with terminated unused lines

An extra feature required in the design is the switched terminating resistors. For SKA requirements the power rating of the resistors can be quite low, some milliwatts. This allows the resistors to be integrated onto the chip at low cost. Existing designs have much higher power ratings leading to higher cost. However, the number of switches needed for a cylindrical reflector SKA should allow a custom design which will keep unit costs low.

The terminating resistors are needed to damp any resonances in the unused delay lines that could cause unwanted frequency response variations. Coupling to the unused delay lines will always occur due to leakage through the OPEN switches, mainly capacitive. With the terminating resistors this leakage power is dissipated and the signal power coupled to the output is approximately the input power multiplied by the isolation of the two series OPEN switches. With switch isolation of 20dB the coupled power is -40dB, which introduces a 0.1dB ripple into the response of the delay element.

GaAs SP4T absorptive switches are already available, for example the 3 GHz MA/COM SW65-0314. But silicon on insulator (SIO) is a promising technology for the high degree of integration required. Current SIO SPDT switches (Peregrine PE4325, $0.93 in quantity) have 0.5dB of attenuation at 3 GHz with isolation greater than 20dB and a return loss of ~18dB. As CMOS technology continues to mature the frequency at which this performance is achieved will continue to grow. Thus the transmission loss through the quad delay element is estimated to be 1dB with a reflection coefficient -15dB. Technology advances may improve on this.

A cascade of two quad delay elements with the first having delay steps of Δ and the second having delay steps of 4Δ allows a total delay range of 15Δ to be spanned. This is sufficient to provide 0.2λ delay steps for the outer feeds of an 8 element line feed. The structure of a possible implementation is shown below. There are on average 3.5 SP4T switches per feed. In volume the estimated current cost of SIO switch is US$2 giving a component cost of US$7 per feed per polarisation. At 1 GHz the switches for dual-polarisation beamforming are estimated to cost US$28 per metre, which is well within the estimated electronics cost of US$115 per metre.

© CSIRO

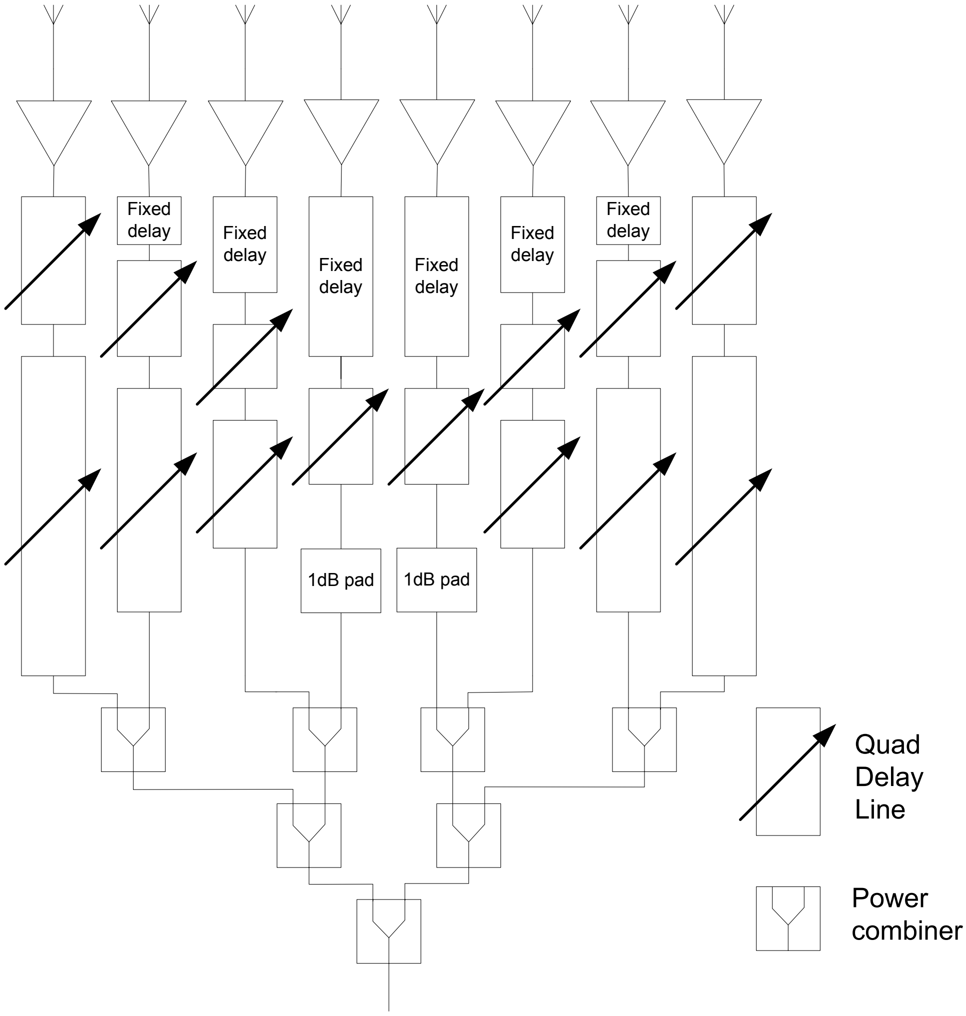

Figure 5 Eight feed RF delay beamformer for 4 GHz operation, length indicates maximum delay of each element.

In this design, feeds are paired symmetrically about the centre. The delay at the array centre is nominally fixed at 1.5λ. For the inner two elements this is achieved with a fixed delay of 1.28λ and a variable delay of up to 0.42λ, which can be implemented with a single quad delay element. All other feeds need two quad delay elements in series together with a fixed delay. Values for these delays are shown below.

Table 4 Delay values for 8 element linefeed beamformer

Feeds	Fixed delay λ	Total variable delay λ	Delays 1st quad delay element λ	Delays 2nd quad delay element λ
1 and 8	0	0 to 3	0, .2, .4, .6	0, .8, 1.6, 2.4
2 and 7	.43	0 to 2.14	0, .14,.28, .43	0, 0.57, 1.14, 1.72
3 and 6	.86	0 to 1.28	0, .09, .18, .27	0, 0.36, 0.72, 1.08
4 and 5	1.28	0 to .42	0, .14, .28, .42	

The maximum delay error for this beamformer is 0.1λ (half a delay step) for the outer feeds. Averaged over all feeds this reduces to 0.07λ or 25°. The balanced nature of the design allows operation of the beamformer with a stable phase centre. If the feeds are taken symmetrically in pairs about the centre then for any pointing the total delay for one feed will be equal 1.5λ plus a steering component. The other feed of the pair will have a delay 1.5λ minus the steering component. When the delay changes both delays

© CSIRO

will move by the same delay but in opposite directions allowing a stable phase centre to be maintained. If other sources of delay and phase error are kept to less than 10% of the step size then the phase error of a pair will be ~2.5° and about 1° when averaged over the four pairs. Beamformers on all the antennas of the central core of the array have the same pointing at any one time. As much of the error is inherent in the design and therefore systematic this reduces the relative errors even further.

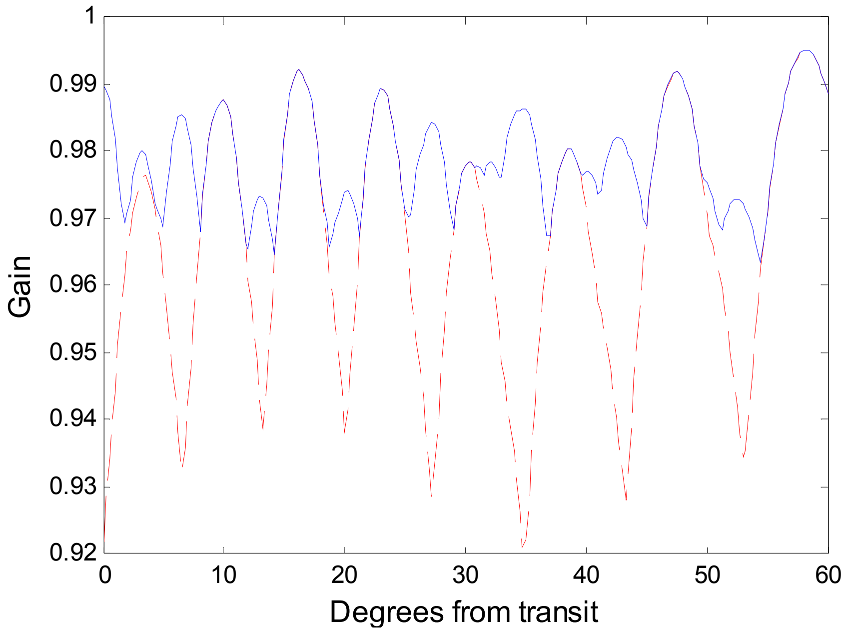

Figure 6 Relative gain of the eight element beamformer

For symmetrical operation the gain of the beamformer versus scan angle is shown above by the dashed line. The mean gain is 0.965 with a standard deviation of 0.02. Allowing non-symmetric operation of the beamformer allows a greater range of phase slopes, which increases the number of pointing directions. This mode of operation introduces known delay offsets that can be removed by later digital processing. The resulting gain versus scan angle is shown by the solid line in the above diagram. The mean gain increases to 0.98 and the standard deviation of the gain reduces to 0.008.

3.3 Q3 Multibeaming

Could the authors clarify the instantaneous sky coverage available and the allowable range of multibeaming within this coverage? Beyond survey work, can the authors expand on other science applications which might justify the complexity of a distributed feed in order to get a constrained multibeaming ability?

At transit the instantaneous sky coverage is defined by the width of the cylinder in declination and in the orthogonal direction (meridian distance MD) by the linefeed. For simplicity, coverage at transit is considered. The transit declination coverage is 1.4°/f where f is the frequency of operation in GHz. In meridian distance the situation is more complicated because the signals from the linefeed can be aggregated in many ways, allowing any instantaneous MD coverage per beam from 120° to 0.125° at 1.4GHz. Further, it is expected that three linefeeds will be active at one time. Pointing for each linefeed is independent of the others, allowing each to have an independent MD.

3.3.1 Line feed signal transmission limitations

On the highest frequencies linefeed, 7 to 22 GHz, there are over 60,000 feed elements in an antenna station linefeed. It is impractical to bring all these back to a central beamformer. Thus, local RF beamforming is performed over 0.3 m sections reducing the number of signals per 100 m linefeed to ~330. The effect of RF beamforming is to reduce the transit MD coverage to $51^o/f$, where f is frequency in GHz. This gives the antenna FOV. Reducing the bandwidth could increase the antenna FOV. This might be difficult to achieve on the highest frequency line feed but on the lower frequency line feeds, below 7 GHz for a 22 GHz SKA, more flexibility is possible.

The full bandwidth is divided into six ~800 MHz IFs. Operating in pairs these can be used to process the signals from the three linefeed elements over 0.3 m and provide full 120^o MD coverage at 1.5 GHz falling to 24^o at 7 GHz.

Table 5 Meridian distance (MD) coverage as a function of frequency *f* GHz

	0.1 to 1.5 GHz	1.5 to 7 GHz	above 7 GHz
MD coverage deg	120	$170/f$	$51/f$
Bandwidth GHz	1.6	1.6	4.9

To take full advantage of this increased sky coverage all the signals from each of the 0.3 m need to be combined in a single beamformer. The total compute power of the beamformer does not change, only its structure. The structure is no longer hierarchical and the amount of data that must be transferred over the fibre from the linefeed to the unified antenna beamformer increases substantially. Each 0.3 m section generates signals for two polarisations at a bit rate of 8 to 16 bits/Hz. Using parallel optical systems such as the Agilent PONI system the cost is about US$30/Gbit/s [10]. The cost of fibre optic electronics is estimated to decrease by a factor of two every two years. This gives a 2010 intra-antenna signal-transport cost, for each antenna, of about US$20,000 per GHz of bandwidth. For the 600 antennas of the SKA this is equal to US$12M/GHz. For convenience the FOV available to the signal transported over the intra-antenna fibre will be referred to as the antenna FOV and is equal to the MD angular coverage multiplied by the beamwidth defined by the reflector.

The above table is for single linefeed operation. With multiple linefeeds operating simultaneously each frequency band is free to point independently in MD. For example, at 1.4 GHz 120^o of MD could be accessible with an 800 MHz bandwidth while at the same time 5^o is accessible at 10 GHz with a 2.4 GHz bandwidth

3.3.2 Imaging FOV

For an antenna within the central core the beamformer reduces the total data rate by a factor of ten. The data rate reduction is greater for long baseline antennas. Half of the reduction is due to changing sampling resolution from 16bits/Hz to 8bits/Hz. Thus the sky coverage, as defined by the signal transmitted from the antenna, is reduced by a factor of five compared to the antenna FOV. The data for this reduced FOV can all be correlated allowing images to be formed. Thus the FOV defined by the antenna-to-correlator bandwidth is the imaging FOV. However, as is shown above, bandwidth can be traded for increased FOV. For example, the full 5^o by 0.14^o of antenna FOV at 20 GHz can be accessed by the correlator if the bandwidth is reduced to ~1GHz. It is only the product of the FOV by the bandwidth that stays constant. FOVs for the cylindrical concept are shown below. Note: below 1.5 GHz the antenna FOV equals the FOV of a linefeed element but the imaging FOV is smaller. Hence the imaging FOV

© CSIRO

can continue to grow quadratically as frequency decreases. Below 0.3 GHz the imaging FOV equals the antenna FOV.

Table 6 Imaging FOV as a function of operating frequency *f* GHz

	0.3 to 1.5GHz	1.5 to 7 GHz	above 7 GHz
MD coverage deg	120	170/*f*	51/*f*
Antnenna FOV deg^2	168/f	238/f^2	72/f^2
Imaging FOV deg^2	48/f^2	48/f^2	15.6/f^2
Bandwidth GHz	1.6	1.6	4.9
FOV *BW deg^2.GHz	76/f^2	76/f^2	76/f^2

This can be compared to 8 deg^2 antenna FOV quoted in the original white paper [1]. At 1.4 GHz this FOV was for the full bandwidth. With a bandwidth of 4.9 GHz the above table still gives 8 deg^2 at 1.4 GHz. With a bandwidth of 800 MHz this increases to 48 deg^2. The table below gives some representative imaging FOVs, see also Figure 2. This FOV is independent of the length of linefeed beamformed, beams that cover the FOV can be fanbeams or circular beams.

Table 7 Imaging FOV for 110 m by 15 m Cylindrical Reflector

	Signal bandwidth GHz		
	0.8	1.6	4.9
Operating frequency GHz	FOV deg^2		
1	96	48	
1.4	48	24	
2	24	12	
3	10.5	5.2	
7	1.9	0.97	0.32
10	0.72*	0.47	0.15
20	0.18*	0.12	0.039

* equal to antenna FOV

3.3.3 Imaging

Imaging 48 deg^2 at 1.4 GHz is no costlier than the 8 deg^2 specified in the original white paper [1]. The original concept allows 64 fanbeams to image 8 deg^2 at 1.4GHz, but the bandwidth of the correlator for a 22 GHz SKA is 4.9 GHz. In trading bandwidth for FOV there are now 384 fanbeams each with 800 MHz bandwidth. This entails no change in the capacity of the correlator or signal transport system. Indeed there is no change to the data flow in the correlator, only the interpretation of the data. In general, if the full length of the linefeed is beamformed into fanbeams then the full antenna FOV can be imaged. If the linefeed is broken up into sections, so as to generate circular beams at transit, then the correlator can image only one eighth of the possible imaging FOV. This may be done to increase spatial dynamic range. The rest of the antenna FOV is still available for other observing modes.

3.3.4 Daily All Sky Monitoring

At 1.4 GHz an 100 MHz-bandwidth, one-minute observation can achieve a sensitivity of ~10 µJy/beam and well over 100 million correlations. The number of correlations is sufficient to provide imaging to a resolution of about 1 arc second within the 48 square degrees of imaging FOV. At this resolution the images will not, in general, be confusion limited allowing all sources to be detected at the ~10 µJy/beam sensitivity. With the one minute integrations the whole visible sky (~30,000 deg^2) can be surveyed

© CSIRO

in about 10.4 hours. The mechanical stress of doing this is low because it is equivalent to approximately four full north-south scans of the antenna. The dead time between observations is small as most of the field changes are electronic and when mechanical changes are needed these are in one degree increments. Dead time could possibly increase the total observing time to 12 hours during the day. The main problem in doing this monitoring is processing the data but continuing advance in processing capabilities will eventually make the program possible.

Other observing will need to proceed as well each day. This will be mainly done in the 12 hours or more per day that is not used by the all sky monitoring. The time available for other observations could be increased to 19 hours if the observing time per pointing was reduced to 15 seconds. Full 5σ sensitivity is still ~20 μJy/beam.

Such a survey would probe new parameter space in both sensitivity and time resolution, and would enable the following key science:

GRBs - The survey would be able to detect the unbeamed radio emission from 'orphan' bursts in which the jet of gamma-rays is pointed away from the observer. Radio afterglows of GRBs typically peak at flux densities of 100-300 μJy for objects at z=1-2 (e.g. Frail et al. 2003 AJ 125, p2299) and can persist for weeks or months. Thus the survey will be able to detect and monitor the radio emission from GRBs out to redshifts as high as z=10.

Radio supernovae in starburst galaxies - The peak radio emission from typical Type II supernovae will be detectable out to redshifts of z=0.2 to 0.5, enabling direct measurements of the supernova rate in starburst galaxies in a way which is unaffected by dust.

AGN variability - The survey will detect quasars, BL Lac objects and similar objects, out to high redshift, by their radio variability. It will also identify and monitor a large numbers of candidate IDV sources whose scintillation can be used to probe the structure of the ISM on scales of microarcsec.

X-ray binaries - The survey will detect the transient radio emission from individual black-hole X-ray binaries in galaxies throughout the Local Group.

Extreme Scattering Events (ESEs) - Characterising the radio-wave lenses which give rise to ESEs requires intensive monitoring programs on large numbers of compact sources. This survey will monitor the fluxes of thousands of quasars and pulsars. Using 'best effort' observing (see section on simultaneous observing) dynamic spectra of hundreds of pulsars can be monitored on a near-daily basis.

3.3.5 Difference imaging

Daily observing will not normally detect fast transients, for these a fast differencing observing mode can be used. Consider two consecutive one-second observations. On baselines up to 4 km the relative position of antennas moves by at most 15 cm per second, about 100th of reflector width. Considering the antenna as a spatial filter this limits the phase change in a correlation to at most 3 degrees. The sidelobes of the dirty beams for the two one-second maps will differ by an estimated 3% and the main lobe will effectively cancel. Thus the difference map has at least 30 times the sensitivity for transient sources where the confusion is due to compact sources. For larger sources the confusion decreases in direct proportion to the area of the sources. The trade-off between differencing images and imaging the differenced UV data is yet to be explored. But, to a first approximation transient sources with a difference flux that is 10^{-6} to 10^{-7}

© CSIRO

less than strongest compact source are detectable. Minimum detectable flux is ~50 μJy allowing **Giant Pulses** to be detected out to about 1 Megaparsec for hourly Crab-type pulses. This approach will also detect prompt radio emission from **GRBs.**

The major advantage that the cylindrical reflector brings to difference imaging is it large FOV. This increases the detection rate by as much as a factor of 30 compared to an instrument with a single 1 square degree FOV.

3.3.6 Simultaneous observing

The cylindrical reflector can be a fast survey instrument. For most other observing programs much of the wide FOV will not be needed. This leaves excess antenna signal bandwidth that can be used to access any of the considerable antenna FOV, e.g. 500 deg^2 at 350 MHz, 120 deg^2 at 1.4 GHz and 0.72 deg^2 at 10 GHz. This extra capacity is ideally suited to searches, for example pulsar, SETI and galaxies in HI that would not be able to exhaust the available sky even in the case of deep field observations.

As an example consider a search for HI in galaxies at redshift z~3. If 60 uniformly distributed fields are selected then one of them will be in the 500 deg^2 of the antenna FOV at any given time. Thus active pointing is not needed. Instead a single beam is dedicated to the search and it observes whichever of the 60 fields falls within the antenna FOV. The 60 fields will each achieve an average of 400 hours of integration in three years without affecting normal targeted observing. This is sufficient to achieve a sensitivity of 10 μJy at a velocity resolution of 20 km/s. At lower redshift the antenna FOV is less and the total integration times lower but the sensitivity is similar because of lower sky noise and wider bandwidths.

This search would obtain redshifts for 100 million or more galaxies and would directly trace the large scale structure of the Universe. These data will also provide a key observational probe of the nature of dark energy. The WMAP results have confirmed a "concordance" cosmological model with a large component of dark energy. The key now is to determine whether the dark energy acts as a "cosmological constant" (w=-1) or "quintessence" (w =fn(z)).

The SKA HI galaxy search would be highly complementary to future optical supernova surveys at high redshift (for example SNAP with 2000 supernovae a z~1.7), in that these experiments adopt different "standard" measurements: supernovae as standard candles versus the sound horizon distance as given between the acoustic peaks in the power spectrum.

The HI galaxy search belongs to a new class of observing, ‘best effort’ observing, that is possible when a very large antenna FOV is available. These observations would be placed on a prioritised list and are observed if they come within the antenna FOV and there is enough antenna bandwidth and backend processing capacity available. Much current observing could be done in this way leaving the SKA free to greatly increase the amount of time critical observing. In terms of science ‘best effort’ observing will allow many more high risk programs. If only one of these extra programs was to make a serendipitous discovery the extra cost of the line feed would be justified. But it must be noted that although the linefeed is costly this is largely offset by the cheapness of the reflector. So in balance there may not be any extra total cost but we may have built a very much faster and versatile instrument. It has a very high survey speed, can perform

© CSIRO

extensive searches, has a much greater chance of making a serendipitous discovery and could still work up to frequencies around 20 GHz.

The alternative view of the large FOV is that it simply increases the speed of the instrument. Compared to a 12 m antenna the speed is 4.6 higher at 20 GHz and 27 times at 1.4 GHz. Increase speed is equivalent to increased sensitivity. Allowing for an effective speed increase of four doubles the sensitivity of the cylindrical reflector to 40,000 m^2/K.

3.4 Q4 Mechanical

Are there lessons which can be learned from existing (or past) cylindrical reflectors in terms of mechanical reliability issues? Are there any new mechanical arrangements envisaged for the SKA implementation?

Cylindrical reflectors can be very reliable. For example Govind Swarup reports that the530 x 30 m Ooty reflector is very reliable since the upgrade to the flexible couplings in the drive shaft, and for the smaller 24x7.5 m 64 reflectors of the N/S arm at Bologna Stelio Montebugnoli states they have worked for more than 35 years with absolutely no problems. The asymmetric E/W arm (35 x 564 m) at Bologna has had problems with the gear boxes but these are now resolved. The lesson here is that greater care must be taken in the design of drive systems for antennas that present asymmetrical load, even partial balancing, such as for Ooty, improves reliability. The other major problem has been snow loading of the antenna. This is also reported by Munetoshi Tokumaru of the STE Laboratory in Nagoya which has 4 cylindrical reflectors (three 100 m x 20 m and one 74 m x 27 m). The high humidity in Japan has also contributed to mechanical failures. This would indicate that the SKA site should be dry and snow free for best reliability. Other problems with the Japanese antenna are due to lighting and power failures which disturb the control system on reflectors with multiple drive systems. This can lead to misalignment between the antenna frames. This suggests that each mechanical unit of the antenna should have a single mechanical drive. Issues with the Molonglo telescope are covered in the original white paper ([1] pages 43-44). In summary, open section structural members are preferred and a single mechanical failure should not cause unrecoverable twisting of the structure.

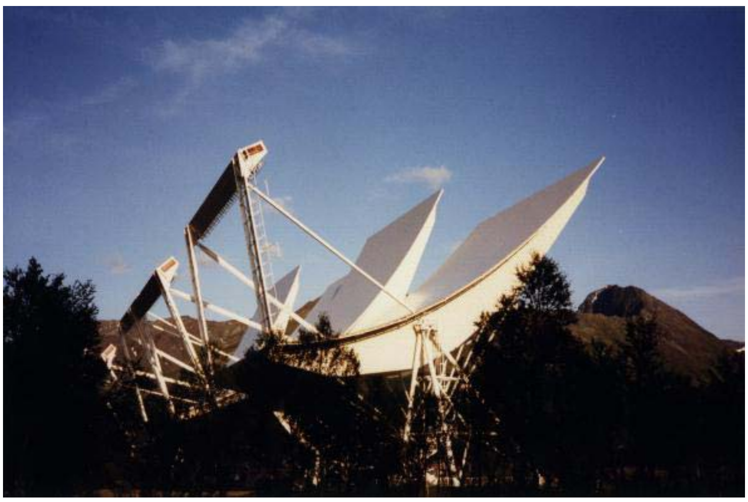

Figure 7 The EISCAT cylindrical reflectors

© CSIRO

For mechanical arrangements the ESICAT antenna [13] provides a prototype that is close to the design proposed in the white paper. This 120 m long by 41m wide antenna is made of four separately steerable elements (above) avoiding drive shaft coupling problems and twisting of the structure. A more radical design could be based on the Solar Trough. These are cylindrical reflectors used for solar energy collection and currently systems have been considered in eight countries of the world, many based on the American LS3 design [11]. The scale of these plants is already at a size comparable to the SKA as is shown in the picture below.

Aerial photo of the SEGS plants in Kramer Junction, California.

The individual reflectors in this system are 100 m long by 5.7 m wide making the existing design close in size to the white paper design. The major innovation used is a single point hydraulic drive, which is illustrated below.

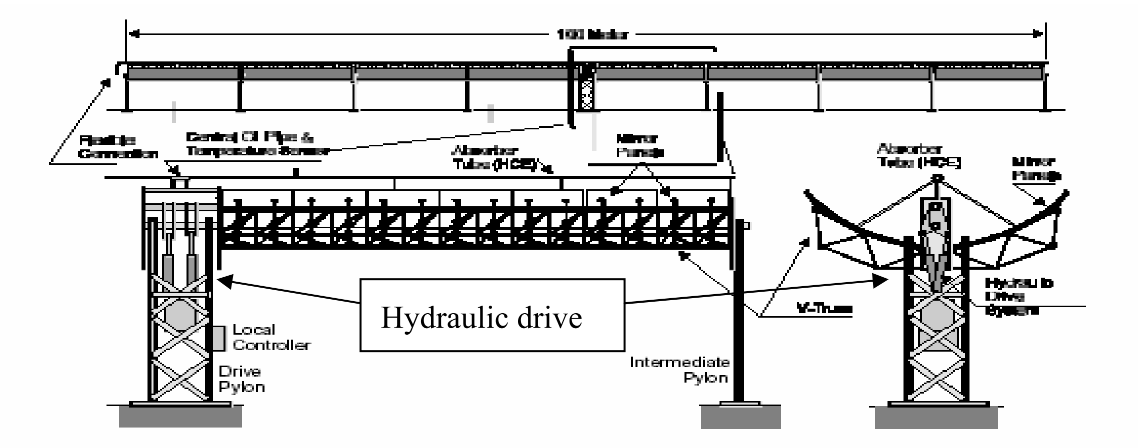

Figure 8 Luz System Three Solar Collector Assembly (LS-3 SCA) from [11]

This shows that a single drive is sufficient to control 50 m of reflector to either side of it. For the SKA, a centralised drive of 25 m section is feasible. The second interesting feature of hydraulic drive is that it allows precise slow motion control with a small low cost motor and hydraulic pump. An extra high power but intermittent operation pump could be used for high speed slewing. A secondary feature of hydraulic drive is fail safe operation by designing the drive so that there is no damage to the surface with hydraulic pistons at the limit of their operation. In effect the mechanical limits of the pistons provide the mechanical limits to the motion.

© CSIRO

The LS3 can also provide cost estimates for a cylindrical reflector. The total cost of 510,000 m^2 solar trough collectors is estimated at US$1,138x80,000 ([11] table 4) giving a cost per square metre of US$178. This is for a structure with a reflecting surface made of mirror glass preformed to a parabolic shape and includes the cost of the absorber tube and couplings. Omitting the absorber tube and the use of a solid aluminium sheet instead of glass would significantly reduce the cost.

The solar trough's RF performance must be estimated to fully compare this technology with the white paper estimates. All of the collected energy is focused onto an absorber tube 7 cm in diameter and there are 4 preformed parabolic reflectors across the width of the reflector, each ~1.5 m wide. For the edge mirrors the absorber subtends an angle of ~1.5 degrees. This corresponds to a mirror tilt of 0.75°. Assuming a setting accuracy of half this then the mirror tilt must be accurate to ±0.2 degrees, equivalent to a ±5 mm. This is a maximum deviation, as a greater deviation would allow solar energy to miss the absorber, which is unacceptable. Thus the surface is probably good to 6 GHz. The white paper estimate for a 5.7 m SKA cylindrical reflector good to 6 GHz is US$123 [1, Appendix I]. This is in good agreement with the solar trough cost estimate after substituting a solid aluminium reflector and subtracting the cost of the absorber tube.

Design work on the backing structure has been undertaken for the EUROTROUGH project [12,13]. The design study concludes that a torsion tube design is best. This concept is basically the same as the spine beam and cantilevered spar design of Molonglo. This confirms the validity of the backing structure concept presented in the white paper.

3.5 Additional questions

Could the authors give a brief outline of any links they see between their concept and potential SKA sites? Issues to consider include:

- *requirements or limitations associated with particular terrain and climate (e.g. need for a given terrain, susceptibility to snow, ice, temperature extremes, high winds, hail and lightning)*

Each antenna requires terrain that is easily graded flat over a 110 metre interval in an east-west direction. All prospective sites, except China, satisfy this requirement. The antenna is robust to most weather extremes. Lightning is a concern requiring careful design of the electronics.

- *approximate energy requirements for central array and remote stations*

The line feed is estimated to need approximately 60mA per dual polarisation LNA. At 22 GHz about 145 are needed per m. Power per metre of linefeed is 9 A @ 2V giving power supply requirement of 40 W per m or 4 kW per antenna at 50% efficiency. The A/D converters and downconverters are the other major power consumer. This may estimated from the 9 W Agilent 20 GS/s converter which is sufficient for 0.3 m of line feed. For the full linefeed at 50% efficiency the power needed is 6 kW. Future devices will be more efficient thus the estimated power consumption is 10-20 kW per antenna / remote station including the beamformer and tracking drive motors. For slewing motors it is suggested that the super capacitors be used to provide peak energy needs. Solar power might be a suitable power source at remote sites in Australia. For the central array the antenna power requirements are 5-10 MW. Many of the proposed sites are near gas pipe lines which could be used as the energy source for a gas turbine generator.

- *requirements related to RF environment (e.g. level of radio quietness demanded by basic system dynamic range)*

Each RF signal path in the cylindrical reflector is connected to the feed with an effective area of 0.3 m by ~12 m, equal to 3.6 m^2. Thus the effective gain of the main beam and near-in sidelobes is low, giving the design better immunity to interference close to the main beam at the expense of greater probability of having an interferer within the main FOV. Even in the main FOV it is estimated that GPS signals will be at 0dB making them easy to deal with. Other satellite systems will exceed the system noise requiring at least 20 dB headroom.

- *requirements for data processing and transport, including any need for local large-scale data processing or aggregation, as well as typical demands on international communications infrastructure (e.g. trans-oceanic fibre)*

Local large-scale data transport is discussed in Q3 above and the processing and aggregation is performed in the beamformer, discussed in the original white paper. International communications is only needed for baselines greater than 3000 km. They would greatly enhance the resolution of the instrument especially if an Australian site is chosen and a number of South Pacific islands are accessible. However, transoceanic links are not essential as standard VLBI recording techniques could be used instead.

The data rate at the output of the correlator should also be considered. With one second integrations it is probably not feasible to transport the raw visibility data over transoceanic links. However within Australia the dedicated fibre network to the long baseline antennas allows the visibility data to be piped to locations close to major cities and universities. It is expected that in ten years time the university/research network will have the capacity, or spare dark fibres, to handle the data, providing the expensive link into major population centres. The alternative is to provide dedicated imaging at the correlator. A full map with spectral data is about 1Tbits, thus with one minute integrations it becomes possible to transport the data over transoceanic links. In most cases only a small fraction of the full 1Tbits is needed. For example, when used for flux monitoring a single value or spectrum is needed, reducing the data rate by many orders of magnitude.

© CSIRO

4 Acknowledgements

The authors would like to thank Michelle Storey and Colin Jacka for checking this document, Mark Walker for his help with Extreme Scattering Events, and Russell Gough and Aaron Chippendale for their input to the discussion on LNAs. The authors would also like to thank the many astronomers who participated in the discussion concerning possible uses of the cylindrical reflectors capability and Ron Ekers for the idea of difference imaging.

5 References

[1] Bunton, J.D., Jackson C.A and Sadler E. M., 'Cylindrical Reflector SKA', SKA memo 23, July 2002. http://www.skatelescope.org/ska_documents.shtml

[2] European SKA Consortium 'Aperture Tile Arrays', SKA memo 19, July 2002. http://www.skatelescope.org/ska_documents.shtml

[3] http://www.toshiba.com/taec/press/to-279.shtml

[4] Shaw, R.D. and Gough, R.G. private communication

[5] Greenberg, D.R, Jagannathan, B., Sweeney, S., Freeman, G and Ahlgren, D., 'Noise Performance of a Low Base Resistance 200 GHz SiGe Technology', IEEE Electron Devices Meeting, Dec 8-11, San Francisco

[6] Bunton, J.D. 'Multi-resolution FX Correlator', Alma memo 447, Feb 2003 http://www.alma.nrao.edu/memos/

[7] SKA specifications from http://www.skatelescope.org/ska_concept.shtml

[8] "compliance" matrix data from the "SKA Designs ("compliance" matrix)" http://www-astro.physics.ox.ac.uk/~sr/ska/ska_matrix.html

[9]James, G.M. & Parfitt, A.J., 'A Low-Cost Cylindrical Reflector for the Square Kilometre Array', in Perspectives on Radio Astronomy: Technologies for Large Antenna Arrays, (eds.) Smolders &. van Haarlem, ASTRON, 1999

[10] http://www.agilent.com/about/newsroom/presrel/2000/13nov2000a.html

[11] http://www.eere.energy.gov/power/pdfs/solar_trough.pdf

[12]Geyer, M., Lüpfert, E., Osuna, R., Esteban A., Schiel, W., Schweitzer, A., Zarza, E., Nava, P., Langenkamp, J., Mandelberg, E., 'EUROTROUGH - Parabolic Trough Collector Developed for Cost Efficient Solar Power Generation' http://www.eurotrough.com/downloads/EuroTroughPaperZurich2002_web.pdf

[13]Kildal Per-Simon, 'Radiation Characteristics of the EISCAT VHF Parabolic Cylindrical Reflector Antenna,' IEEE Trans. Antennas and Propagation, Vol AP-23, No 6, pp 541-561, June 1984

[14] US SKA Consortium, 'The Square Kilometer Array Preliminary Strawman Design Large N - Small D', SKA memo 18, July 2002. http://www.skatelescope.org/ska_documents.shtml

[15] http://www-astro.physics.ox.ac.uk/~sr/ska/ska_matrix.html

Revision History
Submitted 30 May 2003.
Revised June 2003, Table 3 and typographical errors corrected, ISAC reply added.
Revised July 2003, Section 1.5 change to clearly indicate antenna subarraying

© CSIRO

Appendix A: SKA sensitivity

John D. Bunton
CSIRO Telecommunications and Industrial Physics

A.1 Introduction

The SKA flux density sensitivity is a simple function of effective area divided by Tsys. This can then be used to derive the temperature brightness sensitivity. As the array design is independent of antenna selections all concepts with the same Aeff/Tsys will have the same sensitivity. The exceptions are those with very compact cores. Antennas like the LAR can have about ten times the temperature brightness sensitivity on baselines of less than 0.7 km while the cylindrical reflector has three times the sensitivity at baselines less than about 1km.

A.2 Flux Density Sensitivity

The basic equation for the flux density sensitivity ΔS (one sigma) of a synthesis instrument [1] is

$$\Delta S = \frac{2k\,T_{sys}}{A\,\eta_Q \sqrt{n_p [N(N-1)]\Delta\nu\Delta t}}\,\frac{w_{rms}}{w_{mean}} \quad \text{W/m}^2\text{/Hz} \qquad \text{equation 1}$$

where

k is Boltzman constant
Tsys is the system temperature
η_Q is the correlator quantisation efficiency (assumed = 1)
A is the antenna effective area
n_p is the number of simultaneously sampled polarisation (assumed = 2)
N is the number of antennas in the array
$\Delta\nu$ is the bandwidth
Δt is the integration time
w_{mean} is the mean weighting factor over all correlations used to form the image
w_{rmsn} is the rms weighting factor over all correlations used to form the image

This sensitivity is for the case where the detected flux is equal to the rms noise. In practice the five sigma sensitivity is needed. For arrays with a large number of antennas this simplifies to

$$\Delta S_{5\sigma} = \frac{5 \times 2.k\,T_{sys}}{AN\sqrt{2\Delta\nu\Delta t}}\,\frac{w_{rms}}{w_{mean}} \quad \text{W/m}^2\text{/Hz} \qquad \text{equation 2}$$

For the SKA *AN* is the total effective area A_{et}, if *N* is the total number of antennas. For short base lines the mean to rms value is approximately one but only about half the total number of antennas is available. Thus *AN* is equal to $\sim A_{et}/2$. At longer baselines more of the antennas come into play but the mean to rms value decreases if a Gaussian beam is synthesised. For a 'fair' UV distribution [2] *AN* times the mean to rms weighting factor is approximately $A_{et}/2$ greater than the compact core (2 km for the cylindrical reflector). Thus for a Gaussian beam the effective area of the SKA is approximately independent of resolution. If natural weighting of the data is used then the effective area can increase as the baseline increases but a synthesised beam is no longer compact.

© CSIRO

This will cause considerable difficulties in producing a ‘true’ image of the source in the confusion limited regime of the SKA. However, if this problem can be overcome the SKA sensitivity at baselines of 300 m would increase by about 60%. SKA simulations will probably be needed to see if this is possible and for the moment an effective area $A_{et}/2$ is assumed. When this is used equation 2 reduces to:

$$\Delta S_{5\sigma} \approx \frac{T_{sys}}{A_{et}} \frac{20\,k}{\sqrt{2\Delta\nu\Delta t}} \quad \text{W/m}^2\text{/Hz} \qquad \text{equation 3}$$

Thus for the SKA, with A_{et}/Tsys 20,000, this gives a 5 sigma flux density sensitivity of

$$\Delta S_{5\sigma} = \frac{4}{\sqrt{\Delta\nu\Delta t}} \quad \mu\,\text{J}$$

where Δν is measured in GHz and Δt in minutes.

A.3 Brightness Temperature Sensitivity

The brightness temperature sensitivity ΔT can be calculated from the flux density sensitivity [3,4] from

$$\Delta T = \frac{\Delta S \lambda^2}{2k\Omega_s} \ \text{K}$$

where λ is the wavelength and Ω_s is the synthesised beam solid angle

Substituting for ΔS (equation 3) gives a brightness temperature sensitivity of

$$\Delta T_{5\sigma} = \frac{T_{sys}}{A_{et}} \frac{10}{\sqrt{2\Delta\nu\Delta t}} \frac{\lambda^2}{\Omega_s} \ \text{K} \qquad \text{equation 4}$$

A five sigma sensitivity is specified for this parameter [7] at a resolution of 0.1 arcsec for the SKA. The resolution corresponds to a synthesised beam solid angle of $1.85\text{x}10^{-13}$ steradians. For a 12 hour observation the brightness temperature sensitivity given by equation 4 becomes:

$$\Delta T_{5\sigma} = \frac{290\lambda^2}{\sqrt{\Delta\nu}} \ \text{K} \ \text{where } \Delta\nu \text{ is measured in GHz.}$$

For a wavelength of 21 cm the 12-hour SKA brightness temperature sensitivity at 0.1 arcsec is

$$\Delta T_{5\sigma} = \frac{12.8}{\sqrt{\Delta\nu}} \ \text{K} \qquad \Delta\nu \text{ in GHz}$$

The SKA specifications [7] of ΔT=1K at a resolution of 0.1arcsec can be met at 6 GHz or with very long integration at 21cm. Alternatively a 1K five-sigma surface brightness sensitivity at 21 cm is met for resolutions of 0.35 arseconds.

If the synthesised beam can be modelled as a circular Gaussian with beam width

$\theta_s \sim \lambda/B_{max}$ then thesynthesised beam solid angle is given by [3 and 4]:

$$\Omega_s = \frac{\pi}{4\ln(2)}\theta_s^2 \approx \frac{\pi}{4\ln(2)}\frac{\lambda^2}{B_{max}^2} \qquad \text{equation 5}$$

where B_{max} is the maximum baseline. This will be true for the approximation given in equations 3 and 4 where a Gaussian beam is assumed. At λ equal to 21 cm a beam width of 0.1 arcsec corresponds to B_{max} equal to 500 km. Substituting the expression for Ω_s into equation 4 gives

$$\begin{aligned}\Delta T_{5\sigma} &\approx \frac{T_{sys}}{A_{et}}\frac{40\ln(2)}{\pi\sqrt{2\Delta\nu\Delta t}}B_{max}^2 \ \ \mathrm{K} \\ &\approx \frac{T_{sys}}{A_{et}}\frac{6.2}{\sqrt{\Delta\nu\Delta t}}B_{max}^2 \ \ \mathrm{K}\end{aligned} \qquad \text{equation 6}$$

It is seen that for a given maximum baseline the surface brightness sensitivity does not depend on frequency. For a 12 hour observation with a 100 MHz bandwidth on the SKA equation 6 reduces to

$$\Delta T_{5\sigma} \approx 1.5\times10^{-4}\ B_{max}^2\ \ \mathrm{K} \quad \text{where } B_{max} \text{ is in kilometres}$$

Thus a five-sigma brightness temperature sensitivity of 1K is achieved for a 100 MHz bandwidth observation with a maximum baseline of 83 km at 1.4 GHz.

A.4 Alternative Derivation

The brightness temperature sensitivity can be obtained equating the antenna temperature ΔTa to the instrument noise ΔTn [5].

$$\begin{aligned}\Delta Ta &= \eta_a(\Omega s/\Omega p)\Delta Tsky \\ &= \eta_a\left(\left(\frac{\pi\lambda^2}{4\ln(2)B_{max}^2}\right)/\left(\frac{N\lambda^2}{A_{et}}\right)\right)\Delta Tsky \\ &= \eta_a\left(\frac{\pi A_{et}}{4\ln(2)NB_{max}^2}\right)\Delta Tsky\end{aligned}$$

where η_a is the antenna efficiency , Ωs as per equation 5 and Ωp the primary beam of a single antenna is equal to λ^2*N/Aet [6]. The instrument noise is

$$\begin{aligned}\Delta Tn &= \frac{Tsys}{\sqrt{2\Delta\nu\Delta tM}} \\ &\approx \frac{Tsys}{N\sqrt{\Delta\nu\Delta t}}\end{aligned}$$

where M is the number of correlations and is approximately equal to $N^2/2$. Equating the two gives

$$\begin{aligned}\Delta Tsky &= \frac{Tsys}{N\sqrt{\Delta\nu\Delta t}}\frac{4\ln(2)NB_{max}^2}{\pi A_{et}\eta_a} \\ &= \frac{4\ln(2)}{\pi\eta_a}\frac{Tsys}{A_{et}}\frac{B_{max}^2}{\sqrt{\Delta\nu\Delta t}}\end{aligned} \qquad \text{equation 7}$$

© CSIRO

This has the same form as equation 6 but must be increased by five to derive the 5-sigma sensitivity. This makes the constant term approximately 6.8, assuming η_a is approximately 0.65. The constant term in equation 6 is equal to 6.2 thus the two methods are in reasonable agreement.

A.5 Conclusion

Except for the central core, where the filling factor may vary, all SKA concepts will have similar sensitivities. For a one minute observation with a bandwidth of 1 GHz the five sigma flux density sensitivity is 4 μJy, independent of baseline. The brightness temperature sensitivity of 1K at 1.4 GHz is achieved for a 12-hour 100 MHz-bandwidth observation with a maximum baseline of 83 km. For a 21 cm observation this corresponds to a resolution of 0.6 arcseconds.

Acknowledgement

I would like to thank Ravi Subrahmanyan for his help in checking this document.

A.6 References

[1] Thompson, A. R., Moran, J. M. and Swenson, G. W., 'Interferometry and Synthesis in Radio Astronomy', second edition, John Wiley and Sons, Inc, New York, 2001

[2] Bunton, J.D., ' "Fair" UV Coverage for a Multi-Resolution Radiotelescope', SKA workshop, Technology Pathways to the Square Kilometre Array, 3rd-5th August 2000, Jodrell Bank Observatory, UK

[3] 'Synthesis Imaging in Radio Astronomy II', Eds Taylor, Carilli and Perly, Astronomical Society of the Pacific Conference Series, Vol 180, Socorro, USA, 17-23 June, 1988

[4] Butler, B. and Wootten, A., 'ALMA Sensitivity, Supra-THz Windows, and 20 km baselines', ALMA memo No. 267, October 1999,

[5] Subrahmanyan, R. and Ekers, R.D., Sinclair, M. and Silk, J. , 'A search for arcmin-scale anisotropy in the CMB', MNRAS 263, p.416 (1993)

[6] Kraus, J.D. 'Antennas', Second Edition, MacGraw-Hill 1988, ISBN 0-07-100482-3

[7] Ekers, R.D., 'Technical Specifications for the SKA', SKA memo 3, Jan 2002, http://www.skatelescope.org/documents/skamemo3.html

© CSIRO